Bridge-Type SFCL Utilization to Improve the Microgrid Transient Stability and Economic Feasibility

Roy Bayu Negara[1], Fransisco Danang Wijaya[2], Lesnanto Multa Putranto[3], Mohd. Brado Frasetyo[4]

[1,2,3,4] Departemen Teknik Elektro dan Teknologi Informasi, Fakultas Teknik Universitas Gadjah Mada, Jln. Grafika No.2, Kampus UGM, Yogyakarta, 55281, INDONESIA (tel.: 0274-552305; email: [1]roybayunegara92@mail.ugm.ac.id, [2]danangwijaya@ugm.ac.id, [3]lesnanto@ugm.ac.id, [4]mohd.brado41@mail.ugm.ac.id)

ABSTRACT — Currently, renewable energy (RE) generators are widely used by society to reduce emissions. Therefore, a RE-sourced microgrid system coexisting with conventional energy is being developed. However, these electrical energy systems experience transient disturbances such as short circuits, load increase, and decrease in generator output. These disturbances can result in voltage drops and frequency instability. Therefore, efforts are needed to maintain system stability by using a superconducting fault current limiter (SFCL). The SCFL selection is based on its capability to limit the fault current and its speed in providing protection during transient disturbances. The utilized SFCL model is the bridge-type SFCL with two inductors as its main components. Under normal conditions, the current flows through two inductors, and when a fault occurs, the current will go through one inductor. This research was conducted in a scenario where a fault occurred. The voltage value without a bridge-type SFCL during the fault condition was 2.5 V. When a bridge-type SFCL was used, the voltage value was 207 V. Without a bridge-type SFCL, the measured current was 30 kA, whereas the measured current was 1.1 kA with one. The frequency range was 49.7 Hz - 50.2 Hz without bridge-type SFCL and 49.9 Hz - 50.1 Hz with bridge-type SFCL. This research also added an economic feasibility calculation to determine the microgrid system feasibility when using bridge-type SFCL. The calculation consisted of four parts, i.e., net present value (NPV), profitability index (PI), discounted payback period (DPP), and internal rate of return (IRR). Economic feasibility was obtained for an NPV value of US$6,865,405, a PI value of 2.4, a DPP value of four years, and an IRR value of 28.59%. When the obtained value is compared to the feasibility standard, it is determined that a microgrid with SFCL is feasible.

KEYWORDS — Microgrid, Fault, Current Limiter, Renewable Energy, Transient, Bridge-Type SFCL, Economic Feasibility.

I. INTRODUCTION

The current increase in energy demand has adverse impacts on the environment, one of which is the greenhouse gas effect from the use of fossil fuels [1]. Fossil energy use should be discarded because it contributes to global warming, necessitating the use of other energy sources, renewable energy (RE), which is environmentally friendly [2]. The installation of RE-sourced generation on microgrids is on the rise, as is being done in Indonesia, with a target achievement for overall total RE generation by the end of 2025 of 23% [3]. There has been a significant increase in the use of RE sources such as wind energy, both for the environment and for remote area uses [4].

Integrating RE-source energy, such as wind turbines (WT), requires a system, i.e., a microgrid. A microgrid is a group of interconnected loads with various energy resources as a single controllable unit [5]. On the other hand, RE-sourced microgrids are difficult to maintain in a steady state, making them susceptible to disturbances. The causes of disturbances that often occur in the system include short circuits, increased loads, and decreased generator power output or loss. These disturbances are factors leading to transient disturbances. The primary issue in the microgrid is related to the transient disturbance factor, which is to maintain stability after experiencing major disturbances such as short circuit faults, drastic load changes, switching operating modes, and intermittent input power to RE generators. Transient stability is a system's response to a sudden, large disturbance [6]. Thus, the definition of transient stability is the ability of the generator to maintain or continue operation after a disturbance, with circuit faults, line breaks, and generator faults causing transient stability disruptions.

Previous research has found that a superconducting fault current limiter (SFCL) is used to protect a microgrid in suppressing fault currents and compensating for bus voltage drops. The employed SFCL is the resistive type. Furthermore, the outcome of this research is that SFCL can limit the voltage drop and fault current to meet the requirements of fault ride through (FRT) on RE-sourced generators. However, this research employed a parallel-connected grid-connected scenario with a resistive-type SFCL. Therefore, additional testing using the microgrid scenario in the grid-connected state with bridge type SFCL was required [7].

Previous research has concluded that SFCL controls the operation and protects the system when a fault occurs. The employed SFCL was the resistive type. In addition, the outcome of this research is that the SFCL can limit the fault current between distributed generators (DG) and the grid by monitoring the current flow through the installed resistive SFCL. However, this study employed the grid-connected scenario with the SFCL placed between the grid and the DG source. Thus, additional testing was required with the microgrid scenario involving the bridge-type SFCL [8].

Previous research has also found that SFCL controls the operation and protects the system when a fault occurs. The employed current limiter type was the solid-state fault current limiter (SSFCL). Furthermore, the outcome of this research is that the SSFCL can control the fault current with good performance. However, this research only focused on the scenario using a single generator connected to the SSFCL. Therefore, additional testing is required with the microgrid scenario using bridge-type SFCL as well as applications with multiple-generation models [9].

Previous research has also found that SFCL controls the operation and protects the system during a disturbance. The employed SFCL was the resistive type. Furthermore, the outcome of this research is that SFCL can effectively limit the

occurring fault current. However, this study employed the grid-connected condition with resistive-type SFCL placed between the grid and DG source. Thus, additional testing is required with the microgrid scenario under the condition of adding a bridge-type SFCL and calculating the economic feasibility [10].

Based on the results of the conducted search, research on stability in microgrids using current limiters has previously been carried out by several researchers. Currently, the current limiter SFCL, solid-state fault current limiter, electromagnetic fault current limiter, pyrotechnic fault current limiter, and hybrid fault current limiter [11]. In this study, the superconducting SFCL model was selected to be used as the control of transient fault stability. The selection of SFCL was based on its ability to limit fault current as well as its speed in providing protection during transient faults [12]. There are two types of SFCL, i.e., resistors and inductors. Resistor-type SFCL uses resistive components that can withstand current. The weakness of the resistor-type SFCL is that when it reaches its critical temperature, high current flow will cause an increase in temperature, necessitating the use of a cooler. The inductor-type SFCL, however, does not require cooling. Therefore, this study employed an inductor-type SFCL.

The inductor-type SFCL model can overcome the unstable state when a disturbance occurs, especially during transient disturbances, and can also be used as a voltage and frequency stability controller used in the microgrid system.

In this study, the transient stability could be improved from the WT-based microgrid system using an inductor-type SFCL current limiter with a bridge-type configuration. There are two variables to consider when examining microgrid stability. The first variable is the frequency that must be controlled to maintain the stability of the microgrid frequency. The second variable is the voltage must also be controlled to maintain the stability of the microgrid voltage [13], [14]. One of the variables that can be used is the voltage variable which is observed when a power system is operating; then control is carried out to overcome disturbances that can cause the voltage to drop or rise [15]. Thus, this study utilized frequency and voltage variables. The control part used a bridge-type SFCL, which was controlled by a comparator. On the current side, it was measured to see the performance of a bridge-type SFCL that functioned as a current limiter.

II. RESEARCH METHODOLOGY

A. THE FLOW OF CONTROL METHOD DESIGN

The designed control system is a stability control when a transient disturbance occurs in a microgrid. After creating the control system, it can adjust the current amplitude changes occurring in the microgrid. When there is a disturbance, the current amplitude will be high, necessitating a current barrier to prevent surges.

The sensors read the voltage variable when a disturbance occurs so that when there is a decrease or increase outside the standard limits of the State Electricity Company (Perusahaan Listrik Negara, PLN), the SFCL is active. Furthermore, the SFCL becomes a current barrier so that no surges occur. The designed SFCL-type current limiting control scheme has the following stages.

The research was conducted from system design to economic feasibility analysis. The research commenced through system design, where the microgrid system was created using two resources. The first power source came from the power plant, and the second power source was from the WT.
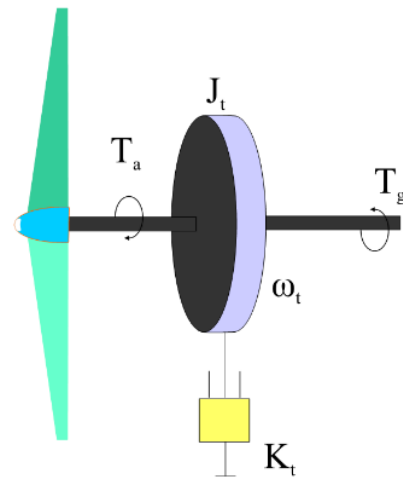

Figure 1. Wind turbine model.

The transient control design was carried out to obtain what components were used as voltage and frequency controllers. After the design stage was carried out, it is found that SFCL can be used as a control. The employed SFCL was a bridge-type SFCL.

After the control and control design was performed, the comparator was added as the next component. The comparator served to analyze the power flow in the system. Comparator reading was only performed on the voltage side as a trigger for the switch contained in the SFCL.

The design stages that had been carried out resulted in microgrid stability. The obtained stability was continued with the calculation of economic feasibility. However, if microgrid stability was not achieved, the design of transient stability controllers was repeated.

B. WIND TURBINE

The components making up the WT for acquiring wind energy consist of the turbine and gearbox, where the use of a gearbox is omitted if the wind turbine uses the direct-connection method (without a gearbox).

Figure 1 shows the WT model; the WT equations can be calculated in (1) and (2).

$$J_t \omega_t = T_a - K_t \omega_t - T_g \tag{1}$$

$$J_t = J_r + n_g^2 J_g \tag{2a}$$

$$K_t = K_r + n_g^2 K_g \tag{2b}$$

$$T_g = n_g T_{em} \tag{2c}$$

where, J_t is the turbine rotor moment of inertia (kg m²); ω_t is the low shaft angular velocity in (rad sec⁻²); K_t is the turbine damping coefficient in (Nm rad⁻¹ sec⁻¹), representing aerodynamic resistance; K_g is the generator damping coefficient in (Nm rad⁻¹ sec⁻¹); representing mechanical friction; J_g is the moment of inertia of the generator rotor (kgm²); T_g is the electromagnetic torque; and T_{em} is the turbine torque (Nm).

The power equation of the mechanical system on the WT can be calculated in (3).

$$P_w = \frac{1}{2} \rho A V_w^3 \tag{3}$$

where, ρ is the air density (kg/m³), A is the blade area (m²), and V is the average wind speed (m/s).

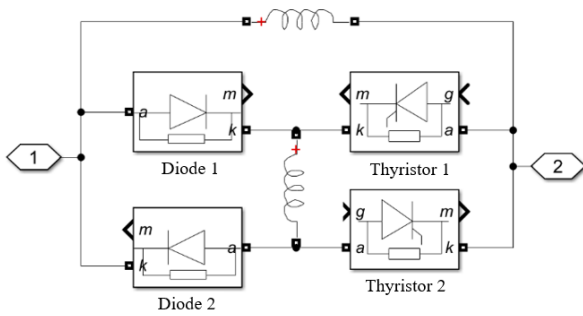The WT has blades with an area that can be calculated using (4).

Figure 2. Bridge-type SFCL connected with a microgrid.

$$A = \pi R^2 \tag{4}$$

where, R is the radius of the turbine (m) and π denotes π constant. The energy that the WT can produce can be calculated in (5).

$$Q_w = P \times time \tag{5}$$

where Q_w is energy (kWh), P is power (W), and *time* is expressed in hours.

The WT converts wind energy by driving a generator to obtain electric current. In this research, an induction generator was used in WT as the electric current generator. The induction generator has a function similar to that of an induction motor, but its operation is distinct; when acting as an induction motor, the rotor rotation speed is slower than the synchronous rotation speed. Furthermore, the induction motor acts as an induction generator if the rotor speed exceeds the synchronous speed. Induction generators and induction motors are reversible [16].

C. SFCL

An SFCL is a control component to limit the fault current in the power system aiming to bind the fault current to prevent voltage drop and frequency fluctuations in the system. Furthermore, SFCL minimizes the occurrence of disturbances by limiting the current value to less than it is prior to the application of SFCL. The selection of SFCL was based on its ability to limit the fault current and speed in providing protection during a fault, especially when experiencing transient conditions.

Figure 2 depicts the form of the SFCL connected to the microgrid through port 1 and port 2. The bridge-type SFCL installation was placed on each line. The placement followed the R, S, and T lines contained in the microgrid system [17]. The primary part of a bridge-type SCFL consists of two inductors, L1 and L2, serving as the paths through which the electric current passes, and they have a switch. The switch serves to activate the line on the L2 inductor. Where, when there is a disturbance in the system, only the L1 inductor receives the current; if no disturbance occurs, both L1 and L2 receive the current. Furthermore, the path on the L1 inductor acting as a limiter was connected in parallel with the L2 inductor.

The form of the SFCL control scheme controlling thyristor 1 and thyristor 2 is depicted in Figure 3. When there is no disturbance, the triggers to thyristor 1 and thyristor 2 gates are active. Meanwhile, when there is a disturbance, thyristors 1 and thyristors 2 are inactive. The detection of transient disturbances on the grid is determined by the voltage on the system with values of higher than 231 and lower than 198. If the voltage exceeds the threshold, then the switch is on. Furthermore, the signal enters the thyristor as a switch to perform switch-on and
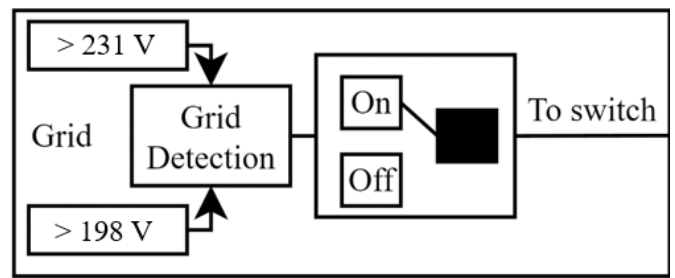

Figure 3. Form of the SFCL control scheme.

turn the thyristor on so that it can activate the limiter to withstand the occurring transient disturbances.

The direction of the current during a disturbance and during normal conditions is different in value. During normal conditions, the current does not surge. Meanwhile, if there is a disturbance, the current suddenly rises and has a very high value. When the current surges, it causes the system to interrupt. A bridge-type SFCL with the configuration of two inductors, two diodes, and two thyristors directs the current flow according to the state of the system. Under normal circumstances, the current flows to both inductors, both diodes, and both thyristors. However, when experiencing a fault, thyristor 1 and thyristor 2 become normally open. Since thyristor 1 and 2 are off, current cannot flow on thyristor 1 and 2. Thus, the current only passes through inductor 1.

The SFCL analysis model assumes the SFCL coil is a solid inductor. Modeling is divided into two operating states: the inductor's state at L1 and the L2 inductor.

The SFCL model used was a bridge-type SFCL. The calculation to determine the inductor value on the SFCL is in (6).

$$X_L = 2\pi \text{ x } f \text{ x } L \tag{6}$$

where, X_L is inductive reactance (ohm), f is the AC frequency of the electrical system (Hz), and L is the coil inductance value (H).

From (6), if the value of L is unknown, then find the value of L using (7).

$$L = \frac{X_L}{2\pi f}. \tag{7}$$

From (7), if the value of X_L is also unknown, then find the value of X_L using (8).

$$X_L = \frac{V}{I} \tag{8}$$

where, V is the system voltage (V) and I is the nominal fault current (A).

D. ECONOMIC FEASIBILITY

The design that was carried out and simulated obtained system stability, necessitating an analysis of the economic feasibility calculation. This analysis is a calculation to determine the feasibility of an investment made in a system design. The project is considered to be feasible if it meets multiple criteria. These criteria are obtained by conducting an analysis in the form of investment feasibility. There are four parts analyzed, i.e., calculating the value of net present value (NPV), profitability index (PI), discounted payback period (DPP), and internal rate of return (IRR).

Calculating investment feasibility by analyzing NPV, PI, DPP, and IRR can be done if it has obtained the values of life
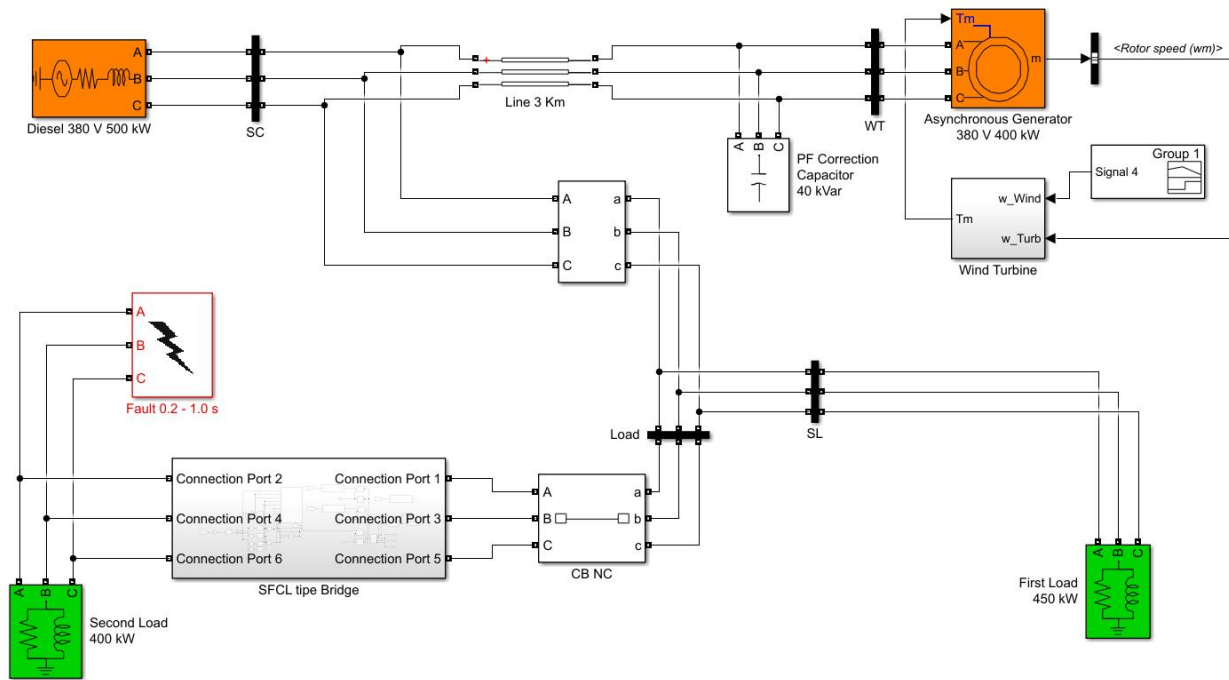
Figure 4. Simulink MATLAB simulation of the proposed model.

cycle cost (LCC) and cost of energy (COE). Life cycle cost can be calculated using (9).

$$LCC = II + O\&M \qquad (9)$$

where, LCC is the life cycle cost, II is the initial investment cost incurred, and $O\&M$ is the cost value of operation and maintenance.

Calculating the LCC value first obtains the P value, where P is the present value of the annual cost over the project's life. The P value calculation can be seen in (10).

$$P = A\left[\frac{(1+i)^n - 1}{i(1+i)^n}\right] \qquad (10)$$

where, A is the annual cost, i is the discount rate, and n is the project life.

The discount rate is future revenue discounted to the present value to be compared to current expenditure. The discount rate refers to the market or bank interest rate. The discount factor calculation can be seen in (11).

$$DF = \frac{1}{(1+i)^n} \qquad (11)$$

where, DF is discount factor.

After that, O&M and present value operation of O&M were calculated based on the O&M cost in one year per kW. The calculation of O&M and O&Mp can be seen in (12).

$$O\&Mp = O\&M\left[\frac{(1+i)^n}{i(1+i)^n}\right] \qquad (12)$$

After the calculation of II and $O\&Mp$ was performed, the LCC value could be calculated. The next calculation after obtaining the LCC value was to find the COE energy cost value. The value of COE or energy costs can be calculated using (13).

$$COE = \frac{LCC \times CRF}{A\ kWh} \qquad (13)$$

where, COE is the cost of energy calculated in rupiah or dollars per kWh, CRF is the capital recovery factor and $A\ kWh$ is the energy generated in one year.
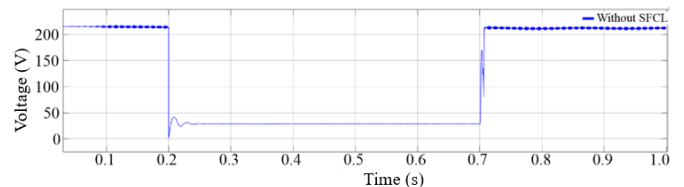

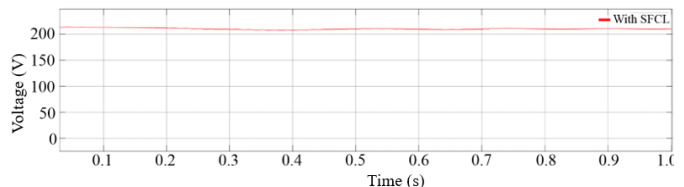**Figure 5.** Voltage when *fault* occurs without bridge-type SFCL.

Figure 6. Voltage when fault occurs using bridge-type SFCL.

After the *LCC* and *COE* values were obtained, the calculation of investment feasibility values could be performed. The NPV, PI, and DPP values can be calculated using (14) to (16).

$$NPV = \sum_{t=1}^{n}\frac{NFC_t}{(1+i)^t} - II \qquad (14)$$

where, NFC_t is the net cash flow from the first year to year n, i is the discount rate, and n is the investment life of n years.

$$PI = \frac{\sum_{t=1}^{n} NFC_t\ (1+i)^{-t}}{II} \qquad (15)$$

$$0 = \sum_{t=0}^{t}\frac{Xt}{(1+IRR)^t} \qquad (16)$$

where, Xt is the cashflow at year t.

If the calculations are made using the above equations, they obtain a value determining the qualification of a project considered to be feasible or not. NPV serves to analyze the entire financial flow based on the discount factor. In the NPV analysis, when a negative value is obtained, the project will be unfeasible, while if the value obtained is positive, the project will be feasible.
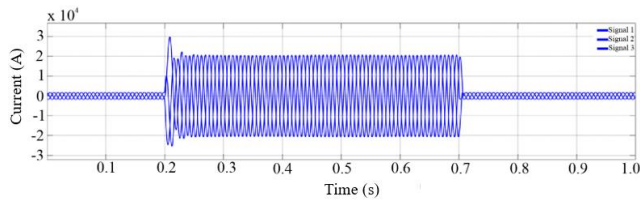
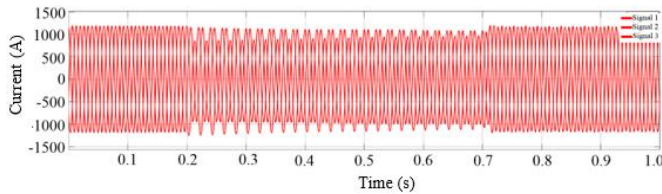**Figure 7.** Current when fault occurs without bridge-type SFCL.

Figure 8. Current when fault occurs using a bridge-type SFCL.

Figure 9. Frequency when fault occurs without bridge-type SFCL

Figure 10. Frequency when fault occurs using a bridge-type SFCL.

The next analysis after calculating the NPV value was to calculate the PI value. The PI value obtained is considered to be feasible if the value is PI > 1. Conversely, if it is not feasible, the value is P < 0. PI has a function to compare the current financial with the initial investment value.

The next analysis after calculating the PI value was to calculate the DPP value. DPP value refers to the project duration (time span) to generate profit when the initial investment value has obtained profit and payback profit has been achieved. If the profit obtained faster than the entire project duration, the investment can be considered to be feasible. Conversely, if the profit obtained exceed the entire project time, the investment can be considered unfeasible.

The next analysis after calculating the DPP value was to calculate the IRR value. The IRR value is a reference to the interest rate level that results in NPV = 0. If the IRR is greater than the initial investment, the project can be considered to be feasible; conversely, if it is smaller than the initial investment, then the project can be considered to be unfeasible.

III. MICROGRID SIMULATION

A. PARAMETERS

The employed components were two generators with a total power of 900 kW, where generator one was a three-phase generator. The three-phase generator was a synchronous generator as the main generator with a capacity of 500 kW connected to the SC bus. Generator two was an induction generator with a capacity of 400 kW. The type of induction generator employed was a squirrel-cage induction generator (SCIG) as a generator in the WT plant.

On the load side, there were two loads with a total load of 850 kW, where the load one totalled 450 kW and load two totalled 400 kW. Furthermore, there was also a bridge-type SFCL as a fault controller. The bridge-type SFCL has internal components consisting of diodes, thyristors, and inductors. The inductor employed a different value between L1 and L2. The value of L1 was greater than that of L2, namely L1 of 0.21 mH and L2 of 0.07 mH.

On the wind resource aspect, wind speed data were obtained, which were used as a reference for calculating the analysis of the economic side; these data were taken from the Ketapang Regency statistical center in 2019 [18].

The parameters used in the simulation refer to the standard rules of PLN's grid code. The value meeting the stability standard of grid code is found in the explanation section of the connection code (CC), if the system frequency can operate
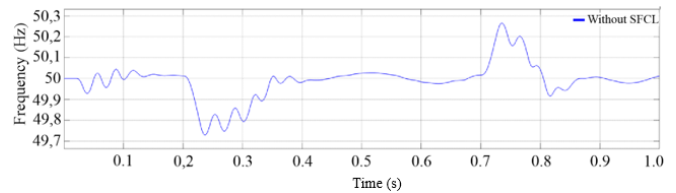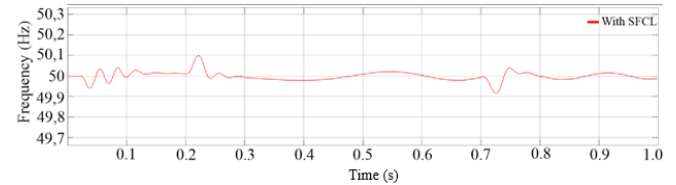
continuously between 49 to 51 Hz [19]. Meanwhile, the reference standard on the voltage side employed PLN Standards of 1995 with a standard voltage variation of 220 V at the upper limit of +5% and -10% at the lower limit [20].

B. SIMULATION FROM SIMULINK MATLAB

System simulation was made using Simulink MATLAB. Figure 4 shows the overall result of the simulation using MATLAB/Simulink. Simulations were performed with a fault scenario. Simulation on microgrid has a test scenario when load two occurs at fault. This scenario was done by making the state fault on load two at 0.2 second to 0.7 second with a simulation for one second.

IV. MICROGRID SIMULATION

A. SIMULATION DISCUSSION USING SIMULINK MATLAB

Voltage standards in accordance with PLN Standards are +5% and -10% of 220 V. The voltage standard for +5% is 231 V for the upper limit and the -10% lower limit is 198 V. The range between 198 V to 231 V is a standard from PLN so that systems can still be categorized as feasible to operate.

Simulation on microgrid used a test scenario when there was fault at the load two. This scenario occurred at 0.2 second to 0.7 second with a one-second simulation.

When a bridge-type SFCL was not used during a fault, it resulted in a voltage drop. The voltage dropped very far below the stability standard. The lowest voltage drop was 2.5 V, and the system could not control the occurring fault because the voltage was too low. Figure 5 shows the voltage when a fault occurs without bridge-type SFCL.

When a bridge-type SFCL was used during the occurrence of a fault, it resulted in stabilizing the voltage in the microgrid system. The voltage was within the standard range of stability allowed when operating. The voltage drop did not occur because the voltage when the fault occurred was 207 V and the system could control that fault. Figure 6 shows the voltage when a fault occurs during the bridge-type SFCL operation.

When the bridge-type SFCL was not used during the occurrence of a fault, it resulted in an increase in current. The current would surge up very high which might result in a disruption of stability. The highest current increase was 30 kA and the system could not control the occurring fault because the current was too high. Figure 7 shows the current when a fault occurs without a bridge-type SFCL.

When a bridge-type SFCL was used during the occurrence of a fault, it would result in the current flow being limited in

Parameters	Values
LCC (USD)	4,879,341
O&M (USD)	463,006
O&Mp (USD)	3,941,834
COE (USD/kWh)	0.078
NPV(USD)	6,865,405
PI	2.4
DPP (Year)	4
IRR (%)	28.59
Wind Average (m/s)	8.5

the microgrid system. The limited current resulted in not very high current surge due to the fault. The current could be limited very significantly with the highest value of 1.1 kA and the system could be controlled because the current had been limited which resulted in no voltage drop. Figure 8 shows the current when a fault occurs using a bridge-type SFCL.

When the bridge-type SFCL was not used during the occurrence of a fault it caused the frequency to fluctuate. The frequency fluctuations were not outside the allowed standards as the lowest value was 49.7 Hz and the highest was 50.2. Hz. Figure 9 shows the frequency when a fault occurs without a bridge-type SFCL.

When the bridge-type SFCL was not used during the occurrence of a fault, it caused the frequency to fluctuate. The frequency fluctuations were not outside the allowed standards as the lowest value was 49.9 Hz and the highest was 50.1 Hz. Figure 10 shows the frequency when a fault occurs without a bridge-type SFCL.

B. ECONOMIC FEASIBILITY DISCUSSION

In this research, economic feasibility was used as a benchmark for a project. The feasibility analysis was tested after all calculations were performed. The calculation starts from the LCC, O&M, O&Mp, COE, NPV, PI, DPP, and IRR values. All of these sections will explain how the results of a project are categorized as feasible or not. The following are the results obtained from the calculations that have been carried out. Table I presents eight types of analysis obtained from the calculation of investment feasibility analysis and wind data from Ketapang Regency in 2019 [18]. Furthermore, Figure 10 is the overall result of the simulation using Simulink MATLAB.

Wind data were used to obtain the average wind speed over a period of one year. After that, from the average wind speed in the span of one year, calculations were made for the power that WT can generate.

The first calculation was the LCC. The LCC value obtained was US$4,879,341, obtained from the summation of the initial investment value and operating and maintenance costs. The O&M value was obtained by calculating the value of operating and maintenance costs with a value of US$463,006. The O&Mp value was obtained by calculating O&M with the project length to be carried out so that a value of US$3,941,834 was obtained. The COE value was obtained from the cycle cost multiplied by the capital recovery factor divided energy (in kWh) generated by the plant.

The next investment feasibility analysis calculation was to calculate the NPV value. The NPV value was obtained from the total profit minus the total investment with a value of US$6,865,405. The value of US$6,865,405 has a positive value,

so the project can be considered to be feasible. The PI value is a profit index value with a value of 2.4. The P > 1, so the project can be considered to be feasible. The DPP value is the time span needed to return the capital with a value of four years of return on capital. The acquisition of a value of four years is an indicator that the feasibility is fulfilled in terms of DPP.

The IRR value is a value to determine the percentage of profit obtained during the project time span with a value of 28.59%. The value of 28.59% has a value greater than 10%, so the project can be considered to be feasible.

V. CONCLUSION

In this research, voltage and frequency become the stability standard in the simulation. Voltage and frequency in the system can be appropriately controlled when using a bridge-type SFCL which is guided by CC and PLN Standards. The conducted scenario is a fault at load two. The scenario that has been made using a bridge-type SFCL is proven to be able to overcome the transient disturbances that occur and allow the voltage and frequency not to go out of the standard operating feasibility. Therefore, the use of bridge-type SFCL can control transient disturbances in the microgrid system well. Then, the fault current can be held back significantly, especially when the occurrence of a fault.

On the other hand, calculations are performed to determine the project's feasibility from an economic perspective when using SFCL. The values of LCC, O&M, O&Mp, COE, NPV, PI, DPP, and IRR are used to calculate the feasibility. The calculated value derived from the values as mentioned earlier indicates that the project qualifies with a feasible outcome.

The economic feasibility of the bridge-type SFCL Has been obtained, so their use is profitable from an economic standpoint. Besides the economic benefit, using bridge-type SFCL also provides the system with greater stability. The economic side is going to be affected if there is a disturbance due to the lack of stability and will experience a loss of revenue (losses) both from the generation side and from the side of the distributed electrical power, resulting in a decrease in the feasibility side's value.

CONFLICT OF INTEREST

The authors declare that the article entitled "Bridge-Type SFCL Utilization to Improve the Microgrid Transient Stability and Economic Feasibility" is written free of conflict of interest.

AUTHOR CONTRIBUTION

Conceptualization, Roy Bayu Negara and Fransisco Danang Wijaya; methodology, Roy Bayu Negara, Fransisco Danang Wijaya, and Lesnanto Multa Putranto; writing-reviewing and editing, Roy Bayu Negara and Mohd. Brado Frasetyo; preparation-writing-original drafting, Roy Bayu Negara; writing-original drafting, Roy Bayu Negara, Fransisco Danang Wijaya, Lesnanto Multa Putranto, and Mohd. Brado Frasetyo; software, Roy Bayu Negara, Fransisco Danang Wijaya, Lesnanto Multa Putranto, and Mohd. Brado Frasetyo.

REFERENCES

[1] "Diseminasi RUPTL 2021-2030," PT PLN (Persero), 2021.

[2] Y. Sawle, S.C. Gupta, and A.K. Bohre, "Review of Hybrid Renewable Energy Systems with Comparative Analysis of Off-Grid Hybrid System," *Renew. Sustain. Energy Rev.*, Vol. 81, pp. 2217–2235, Jan. 2018, doi: 10.1016/j.rser.2017.06.033.

[3] "Rencana Usaha Penyediaan Tenaga Listrik (RUPTL) PT PLN (Persero) 2021-2030," PT. PLN (Persero), 2021.

[4] Y.A. Medvedkina and A.V. Khodochenko, "Renewable Energy and Their Impact on Environmental Pollution in the Context of Globalization," *2020 Int. Multi-Conf. Ind. Eng., Mod. Technol. (FarEastCon)*, 2020, pp. 1–4, doi: 10.1109/FarEastCon50210.2020.9271508.

[5] M. Ahmed, L. Meegahapola, A. Vahidnia, and M. Datta, "Stability and Control Aspects of Microgrid Architectures-A Comprehensive Review," *IEEE Access*, Vol. 8, pp. 144730–144766, Aug. 2020, doi: 10.1109/ACCESS.2020.3014977.

[6] L. Sun, X. Zhao, and Y. Lv, "Stability Analysis and Performance Improvement of Power Sharing Control in Islanded Microgrids," *IEEE Trans. Smart Grid*, Vol. 13, No. 6, pp. 4665–4676, Nov. 2022, doi: 10.1109/TSG.2022.3178593.

[7] L. Chen *et al*., "Application of a Resistive Type Superconducting Fault Current Limiter for a DC Microgrid System," *2018 IEEE Int. Conf. Appl. Supercond., Electromagn. Devices (ASEMD)*, 2018, pp. 1–2, doi: 10.1109/ASEMD.2018.855893.

[8] M.S. Alam *et al.*, "An Efficient Protection and Control Schemes for IBDG System with Resistive Superconducting Current Limiter," *2021 5th Int. Conf. Elect. Eng., Inf. Commun. Technol. (ICEEICT)*, 2021, pp. 1–5, doi: 10.1109/ICEEICT53905.2021.9667917.

[9] M.S. Alam *et al.*, "An Efficient Adjustable Duty Control Based Current Limiter for Grid-Connected Solar PV System," *2021 5th Int. Conf. Elect. Eng., Inf. Commun. Technol. (ICEEICT)*, 2021, pp. 1–5, doi: 10.1109/ICEEICT53905.2021.9667899.

[10] L. Chen *et al*., "Application and Design of a Resistive-Type Superconducting Fault Current Limiter for Efficient Protection of a DC Microgrid," *IEEE Trans. Appl. Supercond.*, Vol. 29, No. 2, pp. 1–7, Mar. 2019, doi: 10.1109/TASC.2018.2882228.

[11] M. Chewale *et al.*, "A Comprehensive Review on Fault Current Limiter for Power Network," *2019 Int. Conf. Recent Adv. Energy-Efficient Comput., Commun. (ICRAECC)*, 2019, pp. 1–7, doi: 10.1109/ICRAECC43874.2019.8995098.

[12] I.K. Okakwu, P.E. Orukpe, and E.A. Ogujor, "Application of Superconducting Fault Current Limiter (SFCL) in Power Systems: A Review," *Eur. J. Eng. Res., Sci.*, Vol. 3, No. 7, pp. 28–32, Jul. 2018, doi: 10.24018/ejeng.2018.3.7.799.

[13] J. Xu, X. Cao, and Z. Hao, "A Droop Control Strategy Based on Synchronous Rectifier to Modulate the Frequency and Voltage in AC Microgrid*," 2019 22nd Int. Conf. Elect. Mach., Syst. (ICEMS)*, 2019, pp. 1–5, doi: 10.1109/ICEMS.2019.8921702.

[14] S. Ullah, L. Khan, I. Sami, and J.-S. Ro, "Voltage/Frequency Regulation with Optimal Load Dispatch in Microgrids Using SMC Based Distributed Cooperative Control," *IEEE Access*, Vol. 10, pp. 64873–64889, Jun. 2022, doi: 10.1109/ACCESS.2022.3183635.

[15] R. Tan, Y. Wang, and S. Zhang, "Coordination Scheme of SFCL and SMES in the DC Microgrid for Fault Current Limiting and Voltage Stability," *2020 IEEE Int. Conf. Appl. Supercond., Electromagn. Devices (ASEMD)*, 2020, pp. 1–2, doi: 10.1109/ASEMD49065.2020.9276114.

[16] I. Boldea, "Electric Generators and Motors: An Overview," *CES Trans. Elect. Mach., Syst.*, Vol. 1, No. 1, pp. 3–14, Mar. 2017, doi: 10.23919/TEMS.2017.7911104.

[17] M. Satish and H.S. Veena, "Transient Stability Enhancement of a Microgrid Consisting of Solar PV and DFIG based Wind Turbine System Using Bridge Type SFCL," *2020 Int. Conf. Smart Technol. Comput. Elect., Electron. (ICSTCEE)*, 2020, pp. 408–411, doi: 10.1109/ICSTCEE49637.2020.9277174.

[18] Badan Pusat Statistik Kabupaten Ketapang, "Rata-rata Kecepatan Angin Kabupaten Ketapang (Knot), 2018-2019," 2020, [Online], https://ketapangkab.bps.go.id/indicator/151/123/1/rata-rata-kecepatan-angin-kabupaten-ketapang.html

[19] "Aturan Jaringan Sistem Tenaga Listrik (Grid Code)," Regulation of the Minister of Energy and Mineral Resources of the Republic of Indonesia, No. 2, 2020.

[20] "Standar-Standar Tegangan," PT PLN (Persero), 1995.